IEEE Access
Multidisciplinary | Rapid Review | Open Access Journal

Received December 14, 2020, accepted December 28, 2020, date of publication December 30, 2020,
date of current version January 8, 2021.

Digital Object Identifier 10.1109/ACCESS.2020.3048130

New Accurate Approximation for Average Error Probability

YASSINE MOUCHTAK AND FAISSAL EL BOUANANI, (Senior Member, IEEE)
ENSIAS College of Engineering, Mohammed V University, Rabat 10000, Morocco
Corresponding author: Faissal El Bouanani (f.elbouanani@um5s.net.ma)

ABSTRACT This paper proposes new accurate approximations for average error probability (AEP) of a communication system employing either M-phase-shift keying (PSK) or differential quaternary PSK with Gray coding (GC-DQPSK) modulation schemes over generalized fading channel. Firstly, new accurate approximations of error probability (EP) of both modulation schemes are derived over additive white Gaussian noise (AWGN) channel. Leveraging the trapezoidal integral method, a tight approximate expression of symbol error probability for M-PSK modulation is presented, while new upper and lower bounds for Marcum Q-function (MQF) of the first order, and subsequently those for bit error probability (BEP) under DQPSK scheme, are proposed. Next, these bounds are linearly combined to propose a highly refined and accurate BE P's approximation. The key idea manifested in the decrease property of modified Bessel function I_v, strongly related to MQF, with its argument v. As an application, these approximations are used to tackle AEP's approximation under $\kappa - \mu$ shadowed fading. Numerical results show the accuracy of the presented approximations compared to the exact ones.

INDEX TERMS Bit error probability, bounds refinement, DQPSK modulation, M-PSK modulation, Marcum Q-function, symbol error rate, upper bound.

I. INTRODUCTION

Wireless technologies are becoming part of our daily lives and their utilization s increase rapidly due to many advantages such as cost-effectiveness, global coverage and flexibility. Nevertheless, these technologies are infected by many phenomena including shadowing which is relatively slow and gives rise to long-term signal variations and multipath fading which is due to constructive and destructive interferences as a result of delayed, diffracted, reflected, and scattered signal components [1]. A great number of communication channels' models have been proposed in the literature to describe either the fading or the joint shadowing/fading phenomena [2]–[5]. Recently, the $\kappa - \mu$ shadowed fading proposed in [6], has attracted a lot of interest due to its versatility and wide applicability in practical scenarios. For instance, it was used for characterizing signal reception in device-to-device communications, body-to-body communications, underwater acoustic, fifth-generation (5G) communications, and satellite communication systems [7]–[11]. In addition, it was shown that numerous statistical models can be derived from the $\kappa - \mu$ shadowed one by setting the parameters to some specific real positive values [12]. Particularly, when the parameters μ and m are integer, such a model is equivalent to what's referred to as composite fading, namely, mixture Gamma distribution [13]. The AEP is a fundamental performance evaluation tool in digital communications, quantifying the reliability of an instantaneous received signal. Furthermore, dealing with the AEP is quite practical in most applications as it states the average performance irrespective of time. Nonetheless, evaluating AEP in closed form remains a big challenge for numerous communication systems because of the complexity of either the end-to-end fading model or the employed modulation technique. Essentially, depending on the employed modulation scheme, EP is provided in either complicated integral form [1] or first-order Marcum Q-function (MQF) and the zeroth-order modified Bessel function (MBF) of the first kind [14] for various M-ary and differential quadrature phase-shift keying (DQPSK) modulation schemes. That integral form can be reexpressed also in terms Gaussian Q-function (GQF), which is not known in closed form. By its turn, the MQF integral-form involves the MBF with exponential term [1], that can be rewritten appropriately as an upper incomplete upper Fox's H-function (UIFH), or equivalently, an infinite summation of the product of upper incomplete Gamma functions [15]. Thus, obtaining AEP requires the

The associate editor coordinating the review of this manuscript and approving it for publication was Maurizio Magarini.

averaging of a UIFH over a generalized fading distribution, which is not evident particularly for fading model with probability density function (PDF) involving the product of exponential and Fox's H- functions (e.g. $\kappa - \mu$ shadowed model). Obviously, deriving accurate bounds or approximations for the AEP is strongly depending on the EP's ones. To this end, several EP's bounds and approximations for the EP are proposed in the literature, for instance, in [16]–[19], numerous bounds for the symbol error probability (SEP) in the case of M-ary PSK modulation are derived in terms of GQF and its powers. Such a function is itself mathematically intractable when involved in complicated integrals resulting from generalized fading distributions. To remedy this problem, several various works deal with simple, and accurate bounds obtained by approximating the SEP for various modulation schemes by the GQF are used when applied to inspect the performance of a communication system experiencing to a particular bivariate-Fox's H-fading model [20], [21]. In contrast, evaluating the performance of GC-DQPSK modulation requires simple bounds or approximate expressions for MQF due to its complicated closed-form and intractability when involved in the computation of AEP [22]–[25]. In [26] and [27], bounds for EP are investigated, while in [28], new lower and upper bounds for EP were proposed, based on which a novel approximation was derived. Despite the good accuracy of the latter's bounds and/or approximation for both MPSK and GC-DQPSK, they remain useless for AEP computation because of their forms' complications.

A. MOTIVATION

The performance of wireless communication systems, with perfect channel state information (CSI) knowledge at the receiver, is widely examined by the scientific community. However, imperfect estimation of channel coefficients is dealt with various practical scenarios, leading to a significant degradation of the system performance. To overcome this limitation, differential modulation (DM) can be considered as an alternative solution particularly for low-power wireless systems, such as wireless sensor networks and relay networks [29]. The main advantage of this scheme is its simplicity of detection due to the unnecessary channel coefficients estimation and tracking, leading to significant reduction in the receiver computational complexity [30], [31]. However, this comes at a cost of higher error rate or lower spectral efficiency. As a result, selecting the most suitable modulation scheme depends on the considered application and both coherent and non-coherent detections. Motivated by this, this paper is devoted to analyzing the performance of two modulation schemes, namely M-PSK and DQPSK over generalized fading model (e.g., $\kappa - \mu$ shadowed fading channel).

B. CONTRIBUTION

Capitalizing on the above, we aim at this work to propose accurate approximations for EP of aforementioned modulation schemes. Specifically, utilizing the trapezoidal integral method, the EP integral form for various M-ary modulation schemes is tightly approximated particularly for M-PSK scheme, while for DQPSK technique, we start by deriving simple lower and upper bounds for EP by bounding MQF, to be used jointly in finding an accurate approximation of the EP. Pointedly, our main key contributions can be summarized as follows

- We propose a new exponential type approximation for the EP applied to M-PSK modulation for an arbitrary fading model by using the trapezoidal technique integral. To the best of the authors' knowledge, such accurate EP's approximation outperforms those presented in the literature,
- We derive new upper and lower bounds of EP in the case of DQPSK modulation and generalized fading model, based on which, an accurate approximation of BEP is proposed,
- As an application, we provide, relying on the two proposed EP's approximations, a tight approximate expression for AEP over $\kappa - \mu$ shadowed fading channel,
- We provide the asymptotic analysis for both forms of AEP and we demonstrate that the diversity order over $\kappa - \mu$ shadowed fading channel remains constant.

Motivated by this introduction, the rest of this paper can be structured as follows. In section II, a new approximation for the first EP form (i.e., M-ary modulation) for an arbitrary fading model is presented for M-PSK while, new lower and upper bound of EP in the case of DQPSK are derived, based on which an accurate approximation for the EP is deduced. In Section III, as an application, the expression of AEP under $\kappa - \mu$ shadowed fading for both modulation schemes is evaluated. In section IV, the respective results are illustrated and verified by comparison with the exact ones using simulation computing. Section V summarizes the main conclusions.

II. BOUNDS ON THE EP

In this section, we propose new approximate expressions for the two potential different forms of EP, namely (i) complicated integral form, and (ii) MQF form, applied to M-PSK and DQPSK modulations with Gray coding, respectively.

A. EP WITH INTEGRAL FORM

Proposition 1: The SEP for M-PSK modulation can be tightly approximated by

$$\widetilde{\mathcal{H}}_1(\gamma) \simeq \sum_{l=1}^{7} \mathcal{A}_l \exp(-\mathcal{B}_l \gamma), \tag{1}$$

while $\mathcal{A}_l$ and $\mathcal{B}_l$ are given in Table 1.

Proof: The SEP for M-PSK modulation is given as [1, Eq. (8.22)]

$$\mathcal{H}_1(\gamma) = \frac{1}{\pi} \int_0^{\frac{M-1}{M}\pi} \exp\left(-\frac{\varrho\gamma}{\sin^2(\theta)}\right) d\theta, \tag{2}$$

with

$$\varrho = \log_2(M) \sin^2\left(\frac{\pi}{M}\right), \tag{3}$$

and γ denotes the signal-to-noise ratio (SNR) per bit.

TABLE 1. The coefficients $\mathcal{A}_l$ and $\mathcal{B}_l$.

l	1	2	3	4	5	6	7
$\mathcal{A}_l$	$\frac{7M-8}{48M}$	$\frac{1}{8}$	$\frac{1}{8}$	$\frac{1}{8}$	$\frac{M-2}{12M}$	$\frac{M-2}{6M}$	$\frac{M-2}{6M}$
$\mathcal{B}_l$	ϱ	2ϱ	$\frac{20\varrho}{3}$	$\frac{20\varrho}{17}$	$\frac{\varrho}{\cos^2(\frac{M-2}{2M}\pi)}$	$\frac{\varrho}{\cos^2(\frac{M-2}{6M}\pi)}$	$\frac{\varrho}{\cos^2(\frac{M-2}{3M}\pi)}$

Subsequently, (2) can be written as

$$\mathcal{H}_1(\gamma) = Q\left(\sqrt{2\varrho\gamma}\right) + \underbrace{\frac{1}{\pi}\int_0^{\frac{M-2}{2M}\pi} \exp\left(-\frac{\varrho\gamma}{\cos^2(t)}\right) dt}_{\mathcal{I}} \quad (4)$$

where $Q(.)$ denotes the Gaussian $Q-$Function [1, Eq. (4.1)].

The integral $\mathcal{I}$ can be approximated using numerical integration rules. The trapezoidal rule for definite integration of an arbitrary function between $[x_0, x_0 + n\phi]$ is given by

$$\int_{x_0}^{x_0+n\phi} f(t)\, dt = \frac{\phi}{2}\left[g_0 + g_n + 2\sum_{i=1}^{n-1} g_i\right], \quad (5)$$

where $g_i = f(x_0 + i\phi)$ for $i = 0..n$, n refers to the number of sub-intervals equally spaced trapeziums, and ϕ defines the spacing. It is worthy to mention that both, the complexity and bounds of such an approximation depend on the number of sub-intervals, namely the greater n is, the tighter the approximation and the higher the evaluation time one. Thus, it is recommended to look for an optimum value of n ensuring a trade-off between the tightness and computational complexity. By substituting $x_0 = 0$, $\phi = \frac{M-2}{2Mn}\pi$ and $f(t) = \exp\left[-\varrho\gamma/\cos^2(t)\right]$, $\left(\text{i.e., } g_i = \exp\left[-\varrho\gamma/\cos^2(i\frac{M-2}{2Mn}\pi)\right]\right)$ in (5), $\mathcal{I}$ can be approximated for $n = 3$ and $n = 4$, respectively, by

$$\mathcal{I}_3 = \frac{M-2}{12M}\left[\exp(-\varrho\gamma) + \exp\left(-\frac{\varrho\gamma}{\cos^2(\frac{M-2}{2M}\pi)}\right)\right] + \frac{M-2}{6M}\left[\exp\left(-\frac{\varrho\gamma}{\cos^2(\frac{M-2}{6M}\pi)}\right) + \exp\left(-\frac{\varrho\gamma}{\cos^2(\frac{M-2}{3M}\pi)}\right)\right], \quad (6)$$

and

$$\mathcal{I}_4 = \frac{M-2}{16M}\left[\exp(-\varrho\gamma) + \exp\left(-\frac{\varrho\gamma}{\cos^2(\frac{M-2}{2M}\pi)}\right)\right] + \frac{M-2}{8M}\left[\exp\left(-\frac{\varrho\gamma}{\cos^2(\frac{M-2}{8M}\pi)}\right) + \exp\left(-\frac{\varrho\gamma}{\cos^2(\frac{M-2}{4M}\pi)}\right) + \exp\left(-\frac{\varrho\gamma}{\cos^2(3\frac{M-2}{8M}\pi)}\right)\right]. \quad (7)$$

Now, using (6), (7), and plugging [32, Eq.(8b)] into (4), $\mathcal{H}_1$ can be approximated by

$$\widetilde{\mathcal{H}}_1 \sim \frac{1}{16}\exp(-\varrho\gamma) + \frac{1}{8}\exp(-2\varrho\gamma) + \frac{1}{8}\exp\left(-\frac{20}{3}\varrho\gamma\right) + \frac{1}{8}\exp\left(-\frac{20}{17}\varrho\gamma\right) + \mathcal{I}_n. \quad (8)$$

Table 2 summarizes the approximated SEP using (8) for $n = 3$ and $n = 4$ and various M-PSK modulation schemes. Further, Eq. (2) has been evaluated using the sub-routine Trapz of Matlab software. Obviously, the absolute error of such an approximation remains negligible for high instantaneous SNR values, while it is below 10^{-3} above SNR $= 0$ dB for both values of n. To this end, and for complexity reducing purposes, we opt, in what follows, for $n = 3$. Accordingly, (1) is attained by combining (6) and (8). ■

B. EP WITH MQF FORM

The bit error probability (BEP) for DQPSK modulation with Gray coding is given by [14]

$$\mathcal{H}_2(\gamma) = Q_1\left(a\sqrt{\gamma}, b\sqrt{\gamma}\right) - \frac{1}{2}I_0\left(\sqrt{2}\gamma\right)\exp(-2\gamma), \quad (9)$$

with $a = \sqrt{2\left(1-\sqrt{0.5}\right)}$, $b = \sqrt{2\left(1+\sqrt{0.5}\right)}$, $I_v(.)$ is the v-th order modified Bessel function of the first kind [15, Eq. (8.431)], and $Q_1(.,.)$ represents the first-order MQF defined as [1, Eq. (4.34)]

$$Q_1(\alpha, \beta) = \int_\beta^\infty t\exp\left(-\frac{t^2+\alpha^2}{2}\right) I_0(\alpha t)\, dt. \quad (10)$$

1) NEW LOWER BOUND FOR BEP

Proposition 2: The BEP for DQPSK modulation with Gray coding can be lower bounded as

$$\mathcal{H}_2(\gamma) \geq \mathcal{L}(\gamma), \quad (11)$$

with

$$\mathcal{L}(\gamma) \triangleq \delta\mathcal{K}(a, b, \gamma) - \frac{1}{2}I_0\left(\sqrt{2}\gamma\right)\exp(-2\gamma), \quad (12)$$

$$\mathcal{K}(a, b, \gamma) = Q\left((b-a)\sqrt{\gamma}\right) - Q\left((b+a)\sqrt{\gamma}\right), \quad (13)$$

and $\delta = \sqrt{\frac{b}{a}}$.

Proof: As I_v is a decreasing function with respect to the index v [33], yields

$$Q_1\left(a\sqrt{\gamma}, b\sqrt{\gamma}\right) \geqslant \mathcal{J}, \quad (14)$$

with

$$\mathcal{J} \triangleq \int_{b\sqrt{\gamma}}^\infty t\exp\left(-\frac{t^2+a^2\gamma}{2}\right) I_{\frac{1}{2}}\left(a\sqrt{\gamma}t\right) dt. \quad (15)$$

TABLE 2. Comparison between the approximate and the exact ASEP for *M*-PSK.

$M=4$								
SEP \ γ		1	2	3	4	5	6	7
$H_1(\gamma)$,Eq. (2)		1.508×10^{-1}	4.494×10^{-2}	1.425×10^{-2}	4.672×10^{-3}	1.565×10^{-3}	5.319×10^{-4}	1.828×10^{-4}
$\widetilde{H}_1(\gamma)$,Eq. (8)	$n=3$	1.501×10^{-1}	4.460×10^{-2}	1.414×10^{-2}	4.642×10^{-3}	1.556×10^{-3}	5.289×10^{-4}	1.816×10^{-4}
	$n=4$	1.505×10^{-1}	4.472×10^{-2}	1.416×10^{-2}	4.645×10^{-3}	1.557×10^{-3}	5.290×10^{-4}	1.816×10^{-4}
$M=8$								
SEP \ γ		2	4	6	8	10	14	16
$H_1(\gamma)$,Eq. (2)		1.849×10^{-1}	6.083×10^{-2}	2.167×10^{-2}	8.018×10^{-3}	3.034×10^{-3}	4.526×10^{-4}	1.772×10^{-4}
$\widetilde{H}_1(\gamma)$,Eq. (8)	$n=3$	1.847×10^{-1}	6.077×10^{-2}	2.156×10^{-2}	7.976×10^{-3}	3.022×10^{-3}	4.504×10^{-4}	1.760×10^{-4}
	$n=4$	1.847×10^{-1}	6.073×10^{-2}	2.158×10^{-2}	7.980×10^{-3}	3.020×10^{-3}	4.501×10^{-4}	1.760×10^{-4}
$M=16$								
SEP \ γ		5	10	20	30	35	40	45
$H_1(\gamma)$,Eq. (2)		2.173×10^{-1}	8.100×10^{-2}	1.360×10^{-2}	2.508×10^{-3}	1.096×10^{-3}	4.832×10^{-4}	2.143×10^{-4}
$\widetilde{H}_1(\gamma)$,Eq. (8)	$n=3$	2.177×10^{-1}	8.072×10^{-2}	1.358×10^{-2}	2.500×10^{-3}	1.091×10^{-3}	4.794×10^{-4}	2.122×10^{-4}
	$n=4$	2.169×10^{-1}	8.091×10^{-2}	1.354×10^{-2}	2.496×10^{-3}	1.091×10^{-3}	4.807×10^{-4}	2.130×10^{-4}

Now applying [15, Eq. (8.431.4)] for $v=\frac{1}{2}$, one can ascertain

$$I_{\frac{1}{2}}\left(a\sqrt{\gamma}t\right)=\frac{2\sinh(a\sqrt{\gamma}t)}{\sqrt{2\pi a\sqrt{\gamma}t}}, \tag{16}$$

where sinh(.) accounts for the hyperbolic sine function.

By plugging (16) into (15) along with the following identity

$$\sinh\left(a\sqrt{\gamma}t\right)=\frac{\exp\left(a\sqrt{\gamma}t\right)-\exp\left(-a\sqrt{\gamma}t\right)}{2}, \tag{17}$$

one can obtain

$$\mathcal{J}\triangleq\frac{1}{\sqrt{2\pi a}}\int_{b\sqrt{\gamma}}^{\infty}\sqrt{\frac{t}{\sqrt{\gamma}}}\left[\begin{array}{c}\exp\left(-\frac{\left(t-a\sqrt{\gamma}\right)^2}{2}\right)\\-\exp\left(-\frac{\left(t+a\sqrt{\gamma}\right)^2}{2}\right)\end{array}\right]dt. \tag{18}$$

Finally, as $t\geq b\sqrt{\gamma}$, yields

$$\begin{aligned}\mathcal{J}&\geq\delta\left[\begin{array}{c}\frac{1}{\sqrt{2\pi}}\int_{b\sqrt{\gamma}}^{\infty}\exp\left(-\frac{\left(t-a\sqrt{\gamma}\right)^2}{2}\right)dt\\-\frac{1}{\sqrt{2\pi}}\int_{b\sqrt{\gamma}}^{\infty}\exp\left(-\frac{\left(t+a\sqrt{\gamma}\right)^2}{2}\right)dt\end{array}\right]\\&=\delta\mathcal{K}(a,b,\gamma),\end{aligned} \tag{19}$$

which concludes the proof. ■

2) NEW UPPER BOUND FOR BEP

Proposition 3: For $\gamma\geq0$, holds

$$\mathcal{H}_2(\gamma)\leq\mathcal{U}(\gamma),$$

with

$$\mathcal{U}(\gamma)\triangleq\frac{1}{\delta}\mathcal{K}(a,b,\gamma)+\frac{1}{2}I_0\left(\sqrt{2}\gamma\right)\exp(-2\gamma). \tag{20}$$

Proof: Relying on (10) and using integration by part by considering $u'(t)=t\exp\left(-\frac{t^2}{2}\right)$ and $w=I_0\left(\sqrt{a}\gamma t\right)$, one can see

$$Q_1\left(a\sqrt{\gamma},b\sqrt{\gamma}\right)=\mathcal{T}+I_0\left(\sqrt{2}\gamma\right)\exp(-2\gamma),$$

with

$$\mathcal{T}=\int_{b\sqrt{\gamma}}^{\infty}a\sqrt{\gamma}\exp\left(-\frac{t^2+a^2\gamma}{2}\right)I_1\left(a\sqrt{\gamma}t\right)dt\cdot \tag{21}$$

Again, by incorporating the inequality $I_1(t)\leq I_{\frac{1}{2}}(t)$ [33], alongside with (16) and (17) into (21), we get

$$\mathcal{T}\leq\sqrt{\frac{a\sqrt{\gamma}}{2\pi}}\int_{b\sqrt{\gamma}}^{\infty}\frac{1}{\sqrt{t}}\left[\begin{array}{c}\exp\left(-\frac{(t-a\sqrt{\gamma})^2}{2}\right)\\-\exp\left(-\frac{(t+a\sqrt{\gamma})^2}{2}\right)\end{array}\right]dt. \tag{22}$$

Moreover, as $t\geq b\sqrt{\gamma}$ in the aforementioned integrand, one can check

$$\mathcal{T}\leq\frac{1}{\delta}\mathcal{K}(a,b,\gamma). \tag{23}$$

Therefore (20) can be inferred from (23) jointly with (13); this completes the proof. ■

3) APPROXIMATE BEP FOR DQPSK

In this part, a tight approximate expression for the BEP under DQPSK scheme is derived based on the two bounds presented above. In a similar manner to the approach followed in [28], the new proposed approximation is a linear combination of the two aforementioned bounds for $\mathcal{H}_2(\gamma)$, namely

$$\widetilde{\mathcal{H}}_2(\gamma)=\widetilde{\chi}(\gamma)\mathcal{U}(\gamma)+(1-\widetilde{\chi}(\gamma))\mathcal{L}(\gamma). \tag{24}$$

Proposition 4: The function $\chi(\gamma)$ can be chosen as

$$\widetilde{\chi}(\gamma)=\mathcal{C}_0\exp(-\mathcal{D}_0\gamma)+\mathcal{C}_1\exp(-\mathcal{D}_1\gamma), \tag{25}$$

where $\mathcal{C}_i$ and $\mathcal{D}_i$ are the best-fit parameters, depending on the SNR interval, summarized in Table 3.

TABLE 3. Optimum values of fitting parameters for different SNR ranges.

SNR range \ $\mathcal{C}_i, \mathcal{D}_i$	$\mathcal{C}_0$	$\mathcal{D}_0$	$\mathcal{C}_1$	$\mathcal{D}_1$
$\gamma < 1$	0.1786	2.903	0.7564	0.1307
$1 \leq \gamma < 8$	0.3798	1.895	0.6183	7.93×10^{-4}
$\gamma > 8$	0.005206	0.2764	0.6146	5.593×10^{-5}

Proof: First, let's define the following function

$$\chi(\gamma) = \frac{\mathcal{H}_2(\gamma) - \mathcal{L}(\gamma)}{\mathcal{U}(\gamma) - \mathcal{L}(\gamma)}. \tag{26}$$

One can check that

$$\mathcal{H}_2(\gamma) = \chi(\gamma)\mathcal{U}(\gamma) + (1 - \chi(\gamma))\mathcal{L}(\gamma). \tag{27}$$

That is, it is sufficient to look for a tight approximation for (26) so as to approximate $\mathcal{H}_2(\gamma)$.

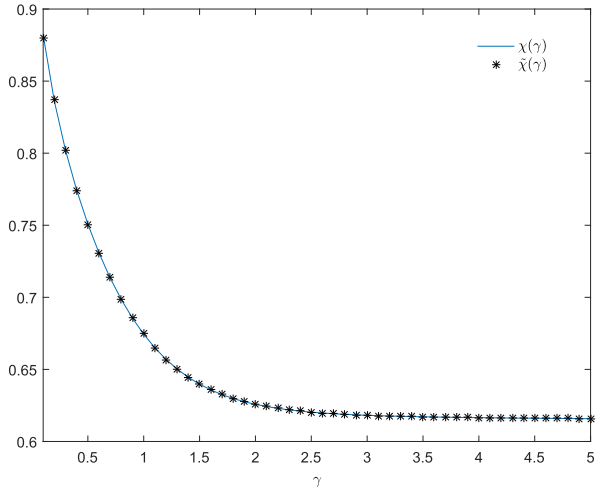

FIGURE 1. Comparison between $\chi(\gamma)$ and $\widetilde{\chi}(\gamma)$.

By plotting $\chi(\gamma)$ as shown in Fig. 1, one can clearly notice its exponential behavior. It follows that its approximate expression can be written in the form (25). Furthermore, the optimized coefficients $\mathcal{C}_i$ and $\mathcal{D}_i$ outlined in Table 3, for various SNR intervals can be straight forward obtained using a curve fitting tool (e.g., Matlab Curve Fitting app); this ends the proof. ■

Remark 1: It is worthwhile that the first-order MQF can be approximated, relying on (9), (12), (20), and (24), by

$$\begin{aligned}\widetilde{\mathcal{Q}}_1\left(a\sqrt{\gamma}, b\sqrt{\gamma}\right) &= \widetilde{\mathcal{H}}_2(\gamma) + \frac{1}{2}I_0\left(\sqrt{2}\gamma\right)\exp(-2\gamma) \\ &= \mathcal{K}(a,b,\gamma)(\eta\widetilde{\chi}(\gamma) + \delta) \\ &\quad + I_0\left(\sqrt{2}\gamma\right)\exp(-2\gamma)\widetilde{\chi}(\gamma), \end{aligned} \tag{28}$$

with

$$\eta = \frac{1 - \delta^2}{\delta}. \tag{29}$$

Both exact and approximate functions $\chi(\gamma)$ and $\widetilde{\chi}(\gamma)$ are plotted in Fig. 1. One can observe that there exists a strong matching between the two curves over the entire range of γ.

Table 4 summarizes the accuracy of the proposed approximation compared with the best ones proposed in the literature, namely $\{\widetilde{\mathcal{H}}_i(\gamma)\}_{i=3..5}$ labeled $\{BER_{i+2}\}_{i=3..5}$ in [28], respectively. Besides, the relative error corresponding to the aforementioned approximations, namely

$$\varepsilon_i = \frac{\left|\widetilde{\mathcal{H}}_i(\gamma) - \mathcal{H}_2(\gamma)\right|}{\mathcal{H}_2(\gamma)}, \quad i = 2..5,$$

is depicted in Fig. 2. Obviously, the relative error corresponding to the proposed approximation outperforms those in [28], except for a short interval, i.e., [11.7, 12.45] where $\mathcal{H}_2(\gamma)$ is negligible, as outlined in Table 2, compared to its values getting for small SNR.

Remark 2: It can be seen clearly that the proposed approximation outperforms the concurrent ones. Moreover, one can check that the three expressions $\{\widetilde{\mathcal{H}}_i(\gamma)\}_{i=3..5}$ are tough, which rend them useless in numerous applications such as the average bit error probability (ABEP) computation under a complicated fading model. Contrarily, the expression of $\widetilde{\mathcal{H}}_2(\gamma)$ is quite simple, making it more appropriate for various fields.

TABLE 4. Comparison between the exact and approximate BEP.

γ	Eq. (9)	$\widetilde{H}_2(\gamma)$, Eq. (24)	$\widetilde{H}_3(\gamma)$, [28]	$\widetilde{H}_4(\gamma)$, [28]	$\widetilde{H}_5(\gamma)$, [28]
0.5	2.6929×10^{-1}	2.6918×10^{-1}	2.7792×10^{-1}	2.6921×10^{-1}	2.6911×10^{-1}
1	1.6391×10^{-1}	1.6395×10^{-1}	1.6383×10^{-1}	1.6383×10^{-1}	1.6568×10^{-1}
1.5	1.0646×10^{-1}	1.0645×10^{-1}	1.0667×10^{-1}	1.0655×10^{-1}	1.0667×10^{-1}
2	7.1611×10^{-2}	7.1614×10^{-2}	7.1685×10^{-2}	7.1625×10^{-2}	7.1885×10^{-2}
2.5	4.9177×10^{-2}	4.9178×10^{-2}	4.9190×10^{-2}	4.9174×10^{-2}	4.9481×10^{-2}
3	3.4227×10^{-2}	3.4226×10^{-2}	3.4228×10^{-2}	3.4226×10^{-2}	3.4482×10^{-2}
4	1.7013×10^{-2}	1.7013×10^{-2}	1.7015×10^{-2}	1.7018×10^{-2}	1.7144×10^{-2}
5	8.6484×10^{-3}	8.6485×10^{-3}	8.6501×10^{-3}	8.6501×10^{-3}	8.7059×10^{-3}
6	4.4613×10^{-3}	4.4613×10^{-3}	4.4624×10^{-3}	4.4617×10^{-3}	4.4859×10^{-3}
7	2.3256×10^{-3}	2.3256×10^{-3}	2.3263×10^{-3}	2.3257×10^{-3}	2.3363×10^{-3}
8	1.2219×10^{-3}	1.2219×10^{-3}	1.2222×10^{-3}	1.2219×10^{-3}	1.2266×10^{-3}
9	6.4596×10^{-4}	6.4597×10^{-4}	6.4613×10^{-4}	6.4597×10^{-4}	6.4594×10^{-4}
10	3.4318×10^{-4}	3.4319×10^{-4}	3.4327×10^{-4}	3.4319×10^{-4}	3.4318×10^{-4}
11	1.8307×10^{-4}	1.8307×10^{-4}	1.8311×10^{-4}	1.8307×10^{-4}	1.8307×10^{-4}
12	9.7990×10^{-5}	9.7990×10^{-5}	9.8011×10^{-5}	9.7990×10^{-5}	9.7990×10^{-5}

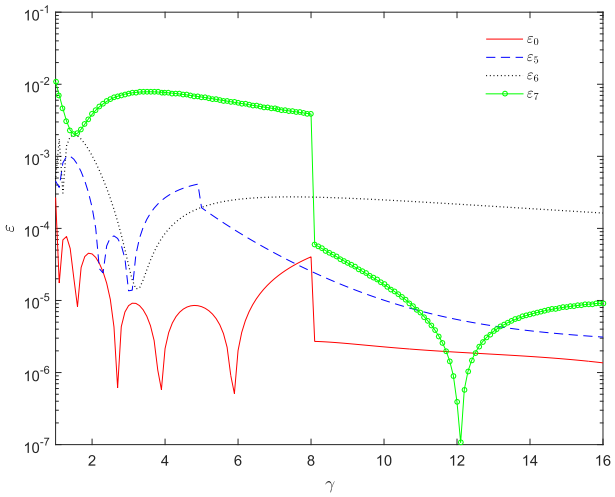

FIGURE 2. Comparison of the relative errors.

III. AEP ANALYSIS

As mentioned above, the proposed approximate EP is used to derive an approximate AEP when communicating over $\kappa-\mu$ shadowed fading.

The PDF of instantaneous SNR γ under the $\kappa-\mu$ shadowed fading model can be written as [12, Eq. 4]

$$f_\gamma(\gamma)=\frac{\lambda}{\Gamma(\mu)}\gamma^{\mu-1}e^{-\nu\gamma}{}_1F_1(m;\mu;\omega\gamma), \tag{30}$$

with

$$\lambda=\frac{\mu^\mu m^m(1+\kappa)^\mu}{\overline{\gamma}^\mu(\mu\kappa+m)^m},\ \nu=\frac{\mu(1+\kappa)}{\overline{\gamma}},\ \omega=\frac{\mu^2\kappa(1+\kappa)}{\overline{\gamma}(\mu\kappa+m)}, \tag{31}$$

where $\overline{\gamma}$ is the average SNR, and when μ is a natural number, it refers to the number of waves' clusters, κ is the ratio between the dominant components' power and the scattered waves' power, while m accounts for the shape parameter. Further, ${}_1F_1(.;.;.)$ and $\Gamma(.)$ denote the Kummer confluent hypergeometric and Euler Gamma functions, respectively.

The AEP approximation for both M-PSK and DQPSK schemes can be straightforwardly evaluated as

$$P_e=\int_0^\infty f_\gamma(\gamma)\,\mathcal{H}_i(\gamma)\,d\gamma, \tag{32}$$

by setting $i=1$ and $i=2$, respectively.

Remark 3: P_e accounts for the average symbol error probability (ASEP) for M-PSK modulation, while it refers to the ABEP for DQPSK modulation with Gray coding.

Proposition 5: In the case of M-PSK modulation, the ASEP over $\kappa-\mu$ shadowed fading model can be approximated as

$$P_e\simeq\lambda\sum_{l=1}^{7}\mathcal{A}_l(\nu+\mathcal{B}_l)^{-\mu}\left(1-\frac{\omega}{\nu+\mathcal{B}_l}\right)^{-m}. \tag{33}$$

Proof: By plugging (1) and (30) in (32) ,and with the help of [15, 7.522 Eq. (9) and 9.121 Eq. (1)] one can obtain (33) . ■

Proposition 6: The ABEP for DQPSK scheme with Gray coding over the $\kappa-\mu$ shadowed fading channel can be tightly approximated as

$$P_e\simeq\frac{\lambda\eta}{\Gamma(\mu)}\sum_{i=0}^{2}\left[\mathcal{C}_i\mathcal{M}_i^{(1)}(a)-\mathcal{C}_i\mathcal{M}_i^{(1)}(-a)+\frac{\mathcal{F}_i}{\eta}\mathcal{M}_i^{(2)}\right], \tag{34}$$

with

$$\mathcal{M}_i^{(1)}(a)=\sum_{k=0}^{\infty}\frac{\phi_{i,k}\,{}_2F_1\left(\frac{1}{2},\mu+k;\mu+k+1;\frac{2\xi_i}{(b-a)^2+2\xi_i}\right)}{2\sqrt{\pi}}, \tag{35}$$

$$\mathcal{M}_i^{(2)}=\sum_{k=0}^{\infty}\psi_{i,k}\,{}_2F_1\left(\frac{\mu+k}{2},\frac{\mu+k+1}{2};1;\frac{2}{(2+\xi_i)^2}\right), \tag{36}$$

$$\phi_{i,k}=\frac{(m)_k\,\omega^k}{(\mu)_k\,k!}\left(\frac{2}{(b-a)^2+2\xi_i}\right)^{\mu+k}\frac{\Gamma\left(\mu+k+\frac{1}{2}\right)}{\mu+k}, \tag{37}$$

$$\psi_{i,k}=\frac{\Gamma(\mu)\,(m)_k\,\omega^k}{k!\,(2+\xi_i)^{\mu+k}}, \tag{38}$$

$$\xi_i=\nu+\mathcal{D}_i, \tag{39}$$

where $(.)_.$ represents the pochhammer symbol, ${}_2F_1(.,.;.;.)$ denotes the hypergeometric functions [15, Eq. (8.310)], $\mathcal{F}_0=\mathcal{C}_0$, $\mathcal{F}_1=\mathcal{C}_1$, $\mathcal{F}_2=-\frac{1}{2}$, $\mathcal{C}_2=\frac{\delta^2}{1-\delta^2}$, and $\mathcal{D}_2=0$.

Remark 4: For Nakagami-m distribution, which is a particular case of $\kappa-\mu$ shadowed RV by setting $\kappa=0$ (i.e., $\omega=0$) and $\mu=m$, $\phi_{i,k}$ and $\psi_{i,k}$ given in (37) and (38), respectively, become

$$\phi_{i,k}=\begin{cases}\left(\frac{2}{(b-a)^2+2\xi_i}\right)^{\mu}\frac{\Gamma\left(\mu+\frac{1}{2}\right)}{\mu}, & k=0\\ 0, & k\neq 0,\end{cases} \tag{40}$$

and

$$\psi_{i,k}=\begin{cases}\frac{\Gamma(\mu)}{(2+\xi_i)^{\mu}}, & k=0\\ 0, & k\neq 0,\end{cases} \tag{41}$$

which means that (35) and (36) will be updated as

$$\mathcal{M}_i^{(1)}(a)=\left(\frac{2}{(b-a)^2+2\xi_i}\right)^{\mu}\frac{\Gamma\left(\mu+\frac{1}{2}\right)}{\mu}\times\frac{{}_2F_1\left(\frac{1}{2},\mu;\mu+1;\frac{2\xi_i}{(b-a)^2+2\xi_i}\right)}{2\sqrt{\pi}}, \tag{42}$$

$$\mathcal{M}_i^{(2)}=\frac{\Gamma(\mu)}{(2+\xi_i)^{\mu}}\,{}_2F_1\left(\frac{\mu}{2},\frac{\mu+1}{2};1;\frac{2}{(2+\xi_i)^2}\right). \tag{43}$$

Proof: First, one can check using (12) and (20) jointly with (13) , (24) , and (25)

$$\widetilde{\mathcal{H}}_2(\gamma)=\eta\sum_{i=0}^{2}\left[\mathcal{C}_i e^{-\mathcal{D}_i\gamma}\mathcal{K}(a,b,\gamma)+\mathcal{F}_i e^{-(2+\mathcal{D}_i)\gamma}I_0\left(\sqrt{2}\gamma\right)\right]. \tag{44}$$

On the other hand, the ABEP for DQPSK can be evaluated as

$$P_e = \int_0^{\infty} f_{\gamma}(\gamma)\, \mathcal{H}_2(\gamma)\, d\gamma. \tag{45}$$

Now, using (30) and (44) in (45), the ABEP can be approximated by

$$P_e \simeq \frac{\lambda\eta}{\Gamma(\mu)} \sum_{i=0}^{2} \left[\mathcal{C}_i \mathcal{M}_i^{(1)}(a) - \mathcal{C}_i \mathcal{M}_i^{(1)}(-a) + \frac{\mathcal{F}_i}{\eta} \mathcal{M}_{i,k}^{(2)} \right], \tag{46}$$

where

$$\mathcal{M}_i^{(1)}(a) = \int_0^{\infty} \gamma^{\mu-1}\, {}_1F_1(m;\mu;\omega\gamma)\, e^{-(\mathcal{D}_i+\nu)\gamma} \times Q\left((b-a)\sqrt{\gamma}\right) d\gamma, \tag{47}$$

and

$$\mathcal{M}_i^{(2)} = \int_0^{\infty} \gamma^{\mu-1}\, {}_1F_1(m;\mu;\omega\gamma)\, e^{-(2+\xi_i)\gamma} I_0\left(\sqrt{2}\gamma\right) d\gamma. \tag{48}$$

Utilizing Craig's formula of the Gaussian Q-function [34, Eq. (5)] and [15, 9.14.1], (47) can be written as

$$\mathcal{M}_i^{(1)}(a) = \sum_{k=0}^{\infty} \frac{(m)_k}{(\mu)_k\, k!} \frac{\omega^k}{\pi} \int_0^{\frac{\pi}{2}} \int_0^{\infty} \gamma^{\mu+k-1} \times \exp\left(-\left(\frac{(b-a)^2}{2\sin^2(\theta)} + \xi_i \right) \gamma \right) d\gamma\, d\theta \tag{49}$$

By evaluating the inner integral in (49) with the aid of [15, Eq. (3.381.4)], we get

$$\begin{aligned} \mathcal{M}_i^{(1)}(a) &= \sum_{k=0}^{\infty} \frac{(m)_k\, \omega^k\, \Gamma(\mu+k) \int_0^{\frac{\pi}{2}} \left(\frac{(b-a)^2}{2\sin^2(\theta)} + 2\xi_i \right)^{-\mu-k} d\theta}{\pi\, (\mu)_k\, k!} \\ &= \sum_{k=0}^{\infty} \frac{(m)_k\, \omega^k\, \Gamma(\mu+k)\, 2^{\mu+k}}{\pi\, (\mu)_k\, k!} \\ &\quad \times \int_0^{\frac{\pi}{2}} \left(\frac{\sin^2(\theta)}{(b-a)^2 + 2\xi_i - 2\xi_i \cos^2(\theta)} \right)^{\mu+k} d\theta \end{aligned} \tag{50}$$

Now, by substituting [15, Eq. (3.682)] into (50), (35) is obtained. Finally, (48) can be evaluated relying on [15, Eqs. (9.14.1) and (6.621.1)] to obtain (36), which concludes the proof. ■

A. ASYMPTOTIC ANALYSIS

In order to gain further insights into system parameters at high SNR regime, an asymptotic analysis for the SNR is carried out. Firstly, note that for large values of $\overline{\gamma}$, one can see that ω goes to 0 and thus the term $k = 0$ dominates the others, ν also goes to 0 (i.e., $\xi_i \simeq \mathcal{D}_i$). It follows that the AEP can be asymptotically approximated as

$$P_e \sim \lambda \sum_{l=1}^{7} \mathcal{A}_l \mathcal{B}_l^{-\mu}. \tag{51}$$

and

$$P_e \sim \frac{\lambda\eta}{\Gamma(\mu)} \sum_{i=0}^{2} \left[\begin{matrix} \mathcal{C}_i \mathcal{M}_i^{(1,asy)}(a) - \mathcal{C}_i \mathcal{M}_i^{(1,asy)}(-a) \\ + \frac{\mathcal{F}_i}{\eta} \mathcal{M}_i^{(2,asy)} \end{matrix} \right], \tag{52}$$

for M-PSK and DQPSK schemes, respectively, with

$$\mathcal{M}_i^{(1,asy)}(a) \sim \Delta\, {}_2F_1\left(\frac{1}{2}, \mu; \mu+1; \frac{2\mathcal{D}_i}{(b-a)^2 + 2\mathcal{D}_i} \right), \tag{53}$$

$$\Delta = \frac{1}{2\sqrt{\pi}} \left(\frac{2}{(b-a)^2 + 2\mathcal{D}_i} \right)^{\mu} \frac{\Gamma\left(\mu+\frac{1}{2}\right)}{\mu}, \tag{54}$$

$$\mathcal{M}_i^{(2,asy)} \sim \frac{\Gamma(\mu)}{(2+\mathcal{D}_i)^{\mu}}\, {}_2F_1\left(\frac{\mu}{2}, \frac{\mu+1}{2}; 1; \frac{2}{(2+\mathcal{D}_i)^2} \right). \tag{55}$$

It is worth mentioning from (51) and (52) alongside with (31) that the diversity order equals μ.

B. BOUND ON THE TRUNCATION ERROR

The above approximate ABEP for DQPSK is expressed in terms of infinite series. Truncating such summation and estimating the truncated error is though of paramount importance for numerical evaluation purposes. In what follows, a closed-form bound for such truncation error is provided.

Using (35), the truncation up to $L-1$ terms of the first summation results to the following error

$$\epsilon_i^{(1)}(a) = \sum_{k=L}^{\infty} \frac{\phi_k}{2\sqrt{\pi}}\, {}_2F_1\left(\frac{1}{2}, \mu+k; \mu+k+1; \frac{2\xi_i}{(b-a)^2+2\xi_i} \right) \tag{56}$$

By changing the summation index to $j = k-L$ in (56), then using [35, Eq. (06.10.02.0001.01)], and performing some manipulations, the bound can be expressed as

$$\epsilon_i^{(1)}(a) \le \frac{\Theta_{i,L}(a)}{2\sqrt{\pi}}\, {}_1F_0\left(\frac{1}{2}; -; \frac{2\xi_i}{(b-a)^2+2\xi_i} \right) \times {}_2F_1\left(1, m+L; L+1; \frac{2\omega}{(b-a)^2+2\xi_i} \right), \tag{57}$$

with

$$\Theta_{i,L}(a) = \left(\frac{2}{(b-a)^2+2\xi_i} \right)^{\mu} \frac{\Gamma(\mu)\,\Gamma(m+L)}{L!\,\Gamma(m)} \times \left(\frac{2\omega}{(b-a)^2+2\xi_i} \right)^{L}. \tag{58}$$

In a similar manner, the truncated error of the summation (36) can be upper bounded by

$$\epsilon_i^{(2)} \le \Lambda_{i,L}\, {}_2F_1\left(\frac{\mu+L}{2}, \frac{\mu+L+1}{2}; 1; \frac{2}{(2+\xi_i)^2} \right) \times {}_2F_1\left(1, m+L; L+1; \frac{\omega}{2+\xi_i} \right), \tag{59}$$

with

$$\Lambda_{i,L} = \frac{\Gamma(\mu)\,\omega^L}{L!\,\Gamma(m+L)\,\Gamma(m)\,(2+\xi_i)^{\mu+L}}. \tag{60}$$

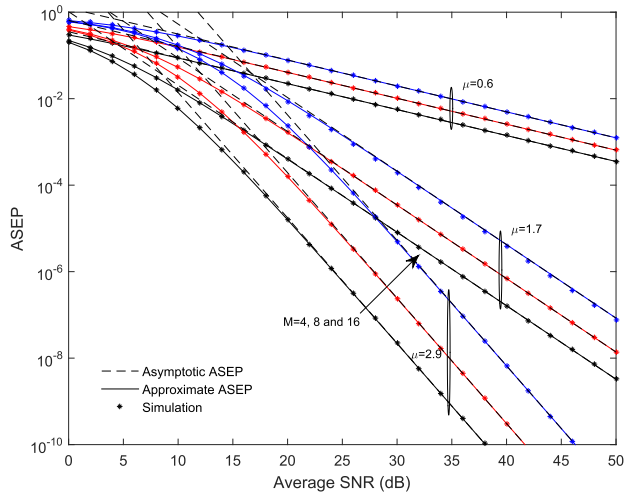

FIGURE 3. ASEP for M-PSK under weak LOS scenario ($\kappa = 1$) with different values of μ and $m = 1.3$.

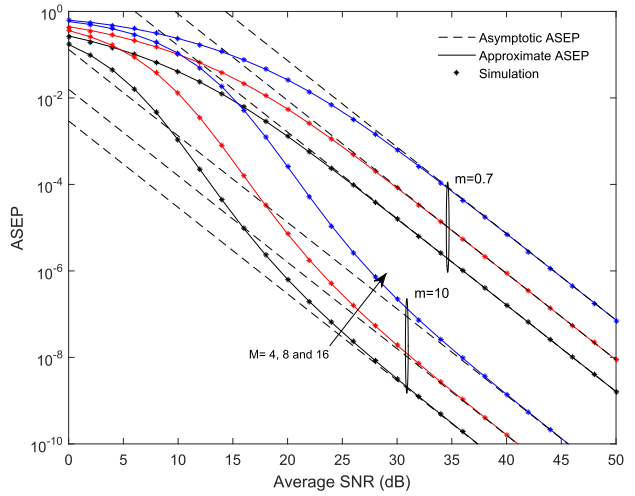

FIGURE 4. ASEP for M-PSK under strong LOS scenario ($\kappa = 10$) with different values of m and $\mu = 2$.

Consequently, and having in mind that $\epsilon_i^{(j)}$ are positives, as can be seen from 57 and 59, the absolute value of the total truncated error can be upper bounded by

$$\left|\epsilon_{P_b}\right| \leq \frac{\lambda\eta}{\Gamma(\mu)} \sum_{i=0}^{2} \left[\mathcal{C}_i \epsilon_i^{(1)}(a) + \mathcal{C}_i \epsilon_i^{(1)}(-a) + \frac{\mathcal{F}_i}{\eta} \epsilon_i^{(2)}\right]. \quad (61)$$

IV. RESULTS AND DISCUSSION

In this section, the proposed approximation for the AEP versus SNR (in dB) of both M-PSK and DQPSK modulations over $\kappa-\mu$ shadowed fading model is evaluated and compared with the exact one for various fading parameters.

Figs. 3 and 7 illustrate, for a fixed value of m, the effect of parameter μ on the AEP for M-PSK and DQPSK modulations, respectively under a weak line of sight (LOS) condition. One can notice that the greater the μ, the better the system's performance.

Figs. 4 and 8 depict the AEP for both modulation schemes under strong LOS ($\kappa = 10$) for a fixed value of μ. It is observed that countering the effect of shadowing requires the increasing of the parameter m.

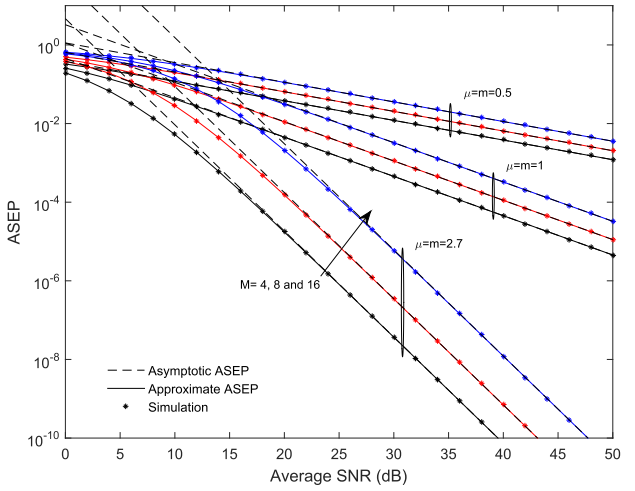

FIGURE 5. ASEP for M-PSK under non-LOS scenario ($\kappa = 0$) with $\mu = m$.

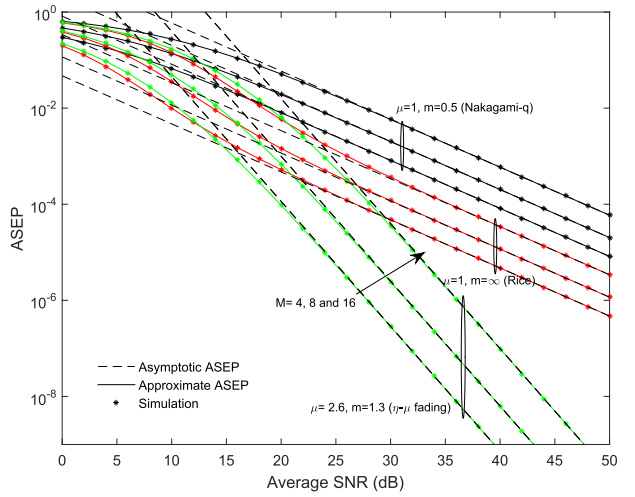

FIGURE 6. ASEP for M-PSK over various practical fading models with $\kappa = 5$.

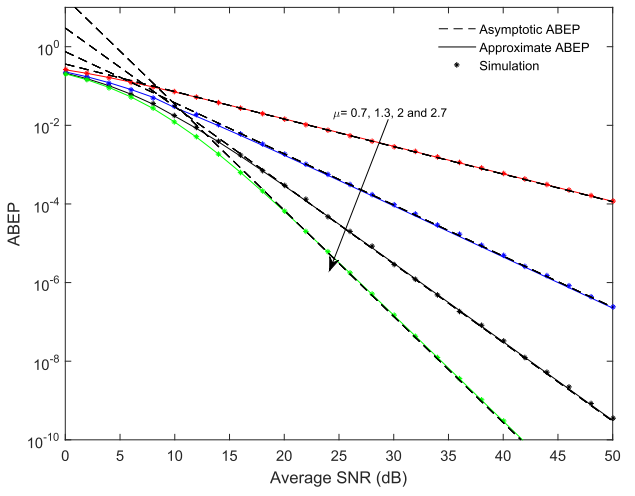

FIGURE 7. ABEP for DQPSK under weak LOS scenario ($\kappa = 1$) with different values of μ and $m = 1.3$.

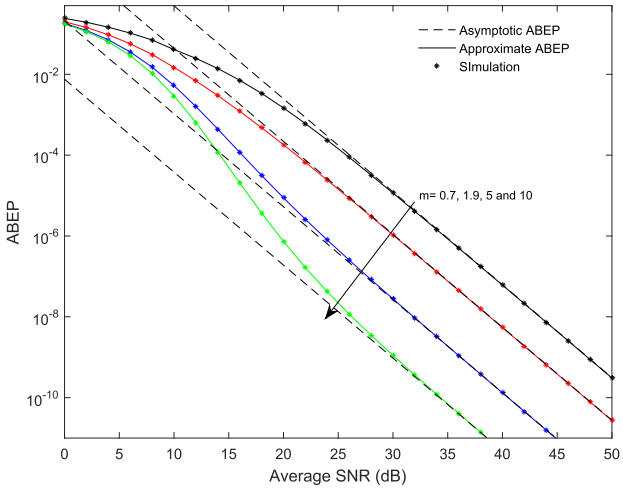

FIGURE 8. ABEP for DQPSK under strong LOS scenario ($\kappa = 10$) with different values of m and $\mu = 2.3$.

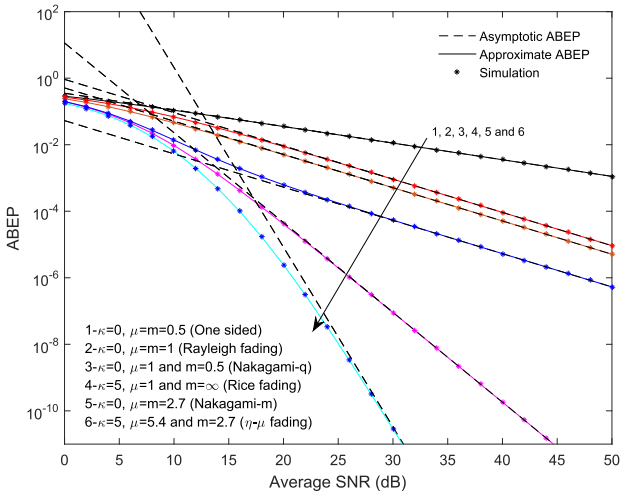

FIGURE 9. ABEP for DQPSK over numerous practical fading distributions with $\kappa = 5$.

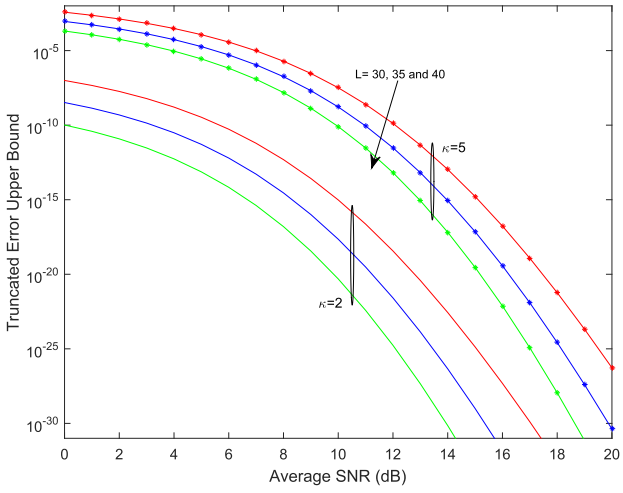

FIGURE 10. Upper bound for the truncated error for $\mu = 2.3$ and $m = 4.7$ and various values of κ and L.

To show the versatility of the $\kappa - \mu$ shadowed fading, Figs. 5, 6, and 9 depict the AEP for some classical

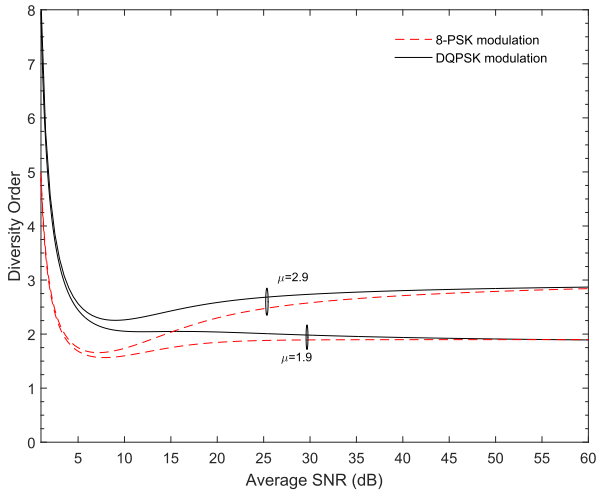

FIGURE 11. Diversity order for $\kappa = 5$, $m = 4.7$ and various values of μ under M-PSK and DQPSK modulation schemes.

fading models. Noteworthy, the results in all figures are provided for either integer or non-integer values of μ and m. Further, the simulation curves match perfectly with the proposed approximation.

Fig. 10 depicts the absolute value of the truncated error versus the number of limited terms L for DQPSK modulation. It can be shown the greater the L, the smaller such error. Interestingly, the truncated error decreases with the increase of SNR.

Lastly, Fig. 11 presents the diversity order for both modulation schemes versus the average SNR is computed by evaluating $-\frac{\log P_e}{\log \bar{\gamma}}$. It is clearly noticed that such metric goes to μ as $\bar{\gamma}$ tends to infinity.

V. CONCLUSION

New approximate expressions for the EP of a communication system employing either M-PSK or DQPSK modulation have been derived. The proposed approximations ensures optimal accuracy-analytical tractability trade-off that enables its versatility to contribute to the AEP computation over generalized fading channel. The resulting accuracy is better than that reached by other existing works relying on more complex mathematical expressions. Furthermore, a new closed-form approximation for the AEP under $\kappa - \mu$ shadowed fading model has been investigated and it is accurate for all the practical values of the SNRs, and are valid for the entire range of the shaping parameters κ, μ, and m. As far as we know, no previous works dealt with such fading and modulation scheme with such a simple approximation.

REFERENCES

[1] M. K. Simon and M.-S. Alouini, *Digital Communication Over Fading Channels*, 2nd ed. Hoboken, NJ, USA: Wiley, 2005.
[2] M. D. Yacoub, "The $\alpha - \mu$ distribution: A physical fading model for the Stacy distribution," *IEEE Trans. Veh. Technol.*, vol. 56, no. 1, pp. 27–34, Jan. 2007.
[3] M. D. Yacoub, "The $\eta - \mu$ distribution and the $\kappa - \mu$ distribution," *IEEE Antennas Propag. Mag.*, vol. 49, no. 1, pp. 68–81, Feb. 2007.

[4] G. Fraidenraich and M. D. Yacoub, "The $\alpha - \eta - \mu$ and $\alpha - \kappa - \mu$ fading distributions," in *Proc. IEEE 9th Int. Symp. Spread Spectr. Techn. Appl.* Manaus, Brazil: Amazon, 2006, pp. 16–20. [Online]. Available: https://ieeexplore.ieee.org/document/4100514, doi: 10.1109/ISSSTA.2006.311725.

[5] R. Cogliatti and R. A. A. de Souza, "A near-100% efficient algorithm for generating $\alpha - \kappa - \mu$ and $\alpha - \eta - \mu$ variates," in *Proc. IEEE 78th Veh. Technol. Conf. (VTC Fall)*, Las Vegas, NV, USA, Sep. 2013, pp. 1–5.

[6] J. F. Paris, "Statistical characterization of $\kappa - \mu$ shadowed fading," *IEEE Trans. Veh. Technol.*, vol. 63, no. 2, pp. 518–526, Feb. 2014.

[7] S. L. Cotton, "Human body shadowing in cellular device to device communications: Channel modeling using the shadowed $\kappa - \mu$ fading model," *IEEE J. Sel. Areas Commun.*, vol. 33, no. 1, pp. 111–119, Jan. 2015.

[8] S. L. Cotton, "Shadowed fading in body-to-body communications channels in an outdoor environment at 2.45 GHz," in *Proc. IEEE-APS Topical Conf. Antennas Propag. Wireless Commun. (APWC)*, Palm Beach, FL, USA, Aug. 2014, pp. 249–252.

[9] F. Cañete, J. López-Fernández, C. García-Corrales, A. Sánchez, E. Robles, F. Rodrigo, and J. Paris, "Measurement and modeling of narrowband channels for ultrasonic underwater communications," *Sensors*, vol. 16, no. 2, p. 256, Feb. 2016.

[10] Y. J. Chun, S. L. Cotton, H. S. Dhillon, F. J. Lopez-Martinez, J. F. Paris, and S. K. Yoo, "A comprehensive analysis of 5G heterogeneous cellular systems operating over $\kappa - \mu$ shadowed fading channels," *IEEE Trans. Wireless Commun.*, vol. 16, no. 11, pp. 6995–7010, Nov. 2017.

[11] J. Zhang, X. Li, I. S. Ansari, Y. Liu, and K. A. Qaraqe, "Performance analysis of dual-hop satellite relaying over $\kappa-\mu$ shadowed fading channels," in *Proc. IEEE Wireless Commun. Netw. Conf. (WCNC)*, San Francisco, CA, USA, Mar. 2017, pp. 1–6, doi: 10.1109/WCNC.2017.7925541.

[12] L. Moreno-Pozas, F. J. Lopez-Martinez, J. F. Paris, and E. Martos-Naya, "The $\kappa - \mu$ shadowed fading model: Unifying the $\kappa - \mu$ and $\eta - \mu$ distributions," *IEEE Trans. Veh. Technol.*, vol. 65, no. 12, pp. 9630–9641, Dec. 2016.

[13] F. J. Lopez-Martinez, J. F. Paris, and J. M. Romero-Jerez, "The κ-μ shadowed fading model with integer fading parameters," *IEEE Trans. Veh. Technol.*, vol. 66, no. 9, pp. 7653–7662, Sep. 2017.

[14] J. G. Proakis, *Digital Communications*, 4th ed. New York, NY, USA: McGraw-Hill, 2001.

[15] A. Jeffrey and D. Zwillinger, *Table of Integrals, Series, and Products*. Amsterdam, The Netherlands: Elsevier, 2007.

[16] C. Chie, "Bounds and approximations for rapid evaluation of coherent MPSK error probabilities," *IEEE Trans. Commun.*, vol. COM-33, no. 3, pp. 271–273, Mar. 1985.

[17] J. J. Komo and K. D. Barnett, "Improved bounds for coherent M-ary PSK symbol error probability," *IEEE Trans. Veh. Technol.*, vol. 46, no. 2, pp. 396–399, May 1997.

[18] S. Park, D. Yoon, and K. Cho, "Tight approximation for coherent MPSK symbol error probability," *Electron. Lett.*, vol. 39, no. 16, pp. 1220–1222, Aug. 2003.

[19] L. Rugini, "SEP bounds for MPSK with low SNR," *IEEE Commun. Lett.*, vol. 24, no. 11, pp. 2473–2477, Nov. 2020, doi: 10.1109/LCOMM.2020.3012837.

[20] F. E. Bouanani, Y. Mouchtak, and G. K. Karagiannidis, "New tight bounds for the Gaussian Q-function and applications," *IEEE Access*, vol. 8, pp. 145037–145055, 2020, doi: 10.1109/ACCESS.2020.3015344.

[21] Y. Mouchtak, F. El Bouanani, and D. B. da Costa, "Tight analytical and asymptotic upper bound for the BER and FER of linear codes over exponentially correlated generalized-fading channels," *IEEE Trans. Commun.*, vol. 67, no. 6, pp. 3852–3864, Jun. 2019.

[22] P. Kam and R. Li, "Computing and bounding the first-order marcum Q-function: A geometric approach," *IEEE Trans. Commun.*, vol. 56, no. 7, pp. 1101–1110, Jul. 2008.

[23] P. Y. Kam and R. Li, "Simple tight exponential bounds on the first-order marcum Q-function via the geometric approach," in *Proc. IEEE Int. Symp. Trans. Inf. Theory*, Seattle, WA, USA, Jul. 2006, pp. 1085–1089.

[24] J. Wang and D. Wu, "Tight bounds for the first order Marcum Q-function," *Wireless Commun. Mobile Comput.*, vol. 12, no. 4, pp. 293–301, Feb. 2012.

[25] X. Zhao, D. Gong, and Y. Li, "Tight geometric bound for marcum Q-function," *Electron. Lett.*, vol. 44, no. 5, pp. 340–341, Feb. 2008.

[26] G. Ferrari and G. E. Corazza, "Tight bounds and accurate approximations for DQPSK transmission bit error rate," *Electron. Lett.*, vol. 40, no. 20, pp. 1284–1285, Sep. 2004.

[27] Y. Sun, A. Baricz, M. Zhao, X. Xu, and S. Zhou, "Approximate average bit error probability for DQPSK over fading channels," *Electron. Lett.*, vol. 45, no. 23, pp. 1177–1179, Nov. 2009.

[28] A. Baricz, S. Andras, and J. Fodor, "New approximations for DQPSK transmission bit error rate," in *Proc. IEEE 8th Int. Symp. Appl. Comput. Intell. Informat. (SACI)*, May 2013, pp. 73–77.

[29] J. Abouei, S. Pasupathy, and K. N. Plataniotis, "Green modulations in energy-constrained wireless sensor networks," *IET Commun.*, vol. 5, no. 2, pp. 240–251, Jan. 2011.

[30] B. Natarajan, C. R. Nassar, and S. Shattil, "CI/FSK: Bandwidth-efficient multicarrier FSK for high performance, high throughput, and enhanced applicability," *IEEE Trans. Commun.*, vol. 52, no. 3, pp. 362–367, Mar. 2004.

[31] F. F. Digham, M.-S. Alouini, and S. Arora, "Variable-rate variable-power non-coherent M-FSK scheme for power limited systems," *IEEE Trans. Wireless Commun.*, vol. 5, no. 6, pp. 1306–1312, Jun. 2006.

[32] D. Sadhwani, R. N. Yadav, and S. Aggarwal, "Tighter bounds on the Gaussian Q-function and its application in Nakagami-m fading channel," *IEEE Wireless Commun. Lett.*, vol. 6, no. 5, pp. 574–577, Jun. 2017.

[33] J. A. Cochran, "The monotonicity of modified bessel functions with respect to their order," *J. Math. Phys.*, vol. 46, nos. 1–4, pp. 220–222, Apr. 1967.

[34] J. W. Craig, "A new, simple and exact result for calculating the probability of error for two-dimensional signal constellations," in *Proc. IEEE Mil. Commun. Conf.*, McLean, VA, USA, Nov. 1991, pp. 571–575.

[35] *Mathematica Edition: Version 12.1*, Wolfram Res., Champaign, IL, USA, 2020.

YASSINE MOUCHTAK was born in Casablanca, Morocco, in 1980. He received the DESA degree from the Faculty of Sciences, Hassan II University, Casa, Morocco, in 2005. He is currently pursuing the Ph.D. degree with the ENSIAS College of engineering, Mohammed V University, Rabat. He has authored publications in well-known conferences and journals, such as IWCMC, PIMRC and the IEEE TRANSACTIONS ON COMMUNICATIONS. His main research interests include the performance analysis and the design of wireless communication systems, signal processing, and information theory.

FAISSAL EL BOUANANI (Senior Member, IEEE) was born in Nador, Morocco, in 1974. He received the M.S. and Ph.D. degrees in network and communication engineering from Mohammed V University–Souissi, Rabat, Morocco, in 2004 and 2009, respectively. He was a Faculty Member with the University of Moulay Ismail, Meknes, from 1997 to 2009. In 2009, he joined the National High School of IT/ENSIAS College of Engineering, Mohammed V University, Rabat, in 2009, where he is currently an Associate Professor. He advised many Ph.D. and master's students at Mohammed V University and the University of Moulay Ismail. So far, his research efforts have culminated in more than 75 papers in a wide variety of international conferences and journals. His current research interests include performance analysis and design of wireless communication systems. He has been involved as a TPC Member in various conferences and IEEE journals. His Ph.D. thesis was awarded the best one by Mohammed V University–Souissi, in 2010. He served as the TPC Chair for the ICSDE conferences and the General Co-Chair for ACOSIS 2016 and CommNet 2018 conferences. He serves as the General Chair for the 2019/2020/2021 CommNet conferences. He is also an Associate Editor of IEEE ACCESS and an Associate Editor of *Frontiers in Communications and Networks* journal. He is also serving as a Lead guest Editor for the Physical Layer Security Special Issue—*Frontiers in Communications and Networks* journal.